BJMS
Borneo Journal of Medical Sciences

ORIGINAL ARTICLE

TP53 Downregulation in Non-melanoma Skin Cancer Cells Treated with *Citrus limon* (Cl) Essential Oil

Muhammad Razin Zamani[1], Wan Fatein Nabeila Wan Omar[2*], Hazulin Mohd Radzuan[2], Muhammad Ashraf Fithri Anuar[3], Muslihah Muzamil[4]

[1]Department of Surgery, Hospital Kajang, 43000 Kajang, Selangor, Malaysia
[2]Department of Basic Medical Sciences, Kulliyyah of Medicine, International Islamic University Malaysia, Jalan Sultan Ahmad Shah, Bandar Indera Mahkota, 25200 Kuantan, Pahang, Malaysia
[3]Department of Surgery, Hospital Segamat, KM6, Jalan Genuang, Bandar Putra, 85000 Segamat, Johor
[4]Department of Internal Medicine, Hospital Queen Elizabeth, Karung Berkunci No. 2029, 88586 Kota Kinabalu, Sabah, Malaysia.

*Corresponding author's email: fateinwanomar@iium.edu.my

Received: 07 July 2025

Accepted: 24 November 2025

Published: 05 September 2026

DOI: https://doi.org/10.51200/bjms.v20i3.6604

Keywords: *Antineoplastic, natural products, skin neoplasms, phytogenic, antiproliferative*

ABSTRACT

Citrus limon essential oil (CLEO) is rich in bioactive compounds, exhibit various therapeutic properties, including anticancer potential. Non-melanoma skin cancers, such as squamous cell carcinoma, are commonly associated with *TP53* mutations, leading to uncontrolled cell proliferation. This study investigates the cytotoxic effects of CLEO on normal human foreskin fibroblast cells (HFF1) and human squamous carcinoma cells (A431) by analysing morphological changes, p53 protein secretion, and *TP53* gene expression. HFF1 and A431 cells were treated with CLEO at concentrations of 125, 250, and 500 µg/mL for 24 hours. Morphological changes were observed using an inverted light microscope, while p53 protein secretion was analysed via Western blot. *TP53* gene expression was assessed using quantitative real-time PCR. Mild structural changes were observed in HFF1 cells at higher CLEO concentrations (250 and 500 µg/mL), whereas A431 cells exhibited significant membrane blebbing and detachment at all concentrations (125, 250, and 500 µg/mL). p53 protein secretion in the culture media increased in HFF1 cells following CLEO treatment, while A431 cells exhibited a dose-dependent reduction in p53 secretion. Additionally, *TP53* gene expression was notably downregulated in A431 cells at 125 and 500 µg/mL CLEO concentrations, suggesting the presence of alternative cytotoxic mechanisms. CLEO shows stronger cytotoxicity against A431 squamous carcinoma cells than against normal

HFF1 fibroblasts, suggesting therapeutic potential. The modulation of p53 protein secretion and *TP53* gene expression suggests that p53 operates through both dependent and independent mechanisms. Further studies, including in vivo and clinical investigations, are needed before its application in cancer therapy can be considered.

INTRODUCTION

Citrus limon (CL), also known as lemon, belongs to the genus *Citrus*, a part of the Rutaceae family. It is widely used in the food, cosmetic and cleaning products industries. The fruits are the primary raw material used to extract juice and essential oil (EO). While CL juice is rich in flavonoids, phenolic acids and vitamins, CL essential oil (CLEO) contains monoterpenoids, furanocoumarins and polymethoxylated flavones. Limonene is the most dominant monoterpenoid in CLEO (Klimek-szczykutowicz et al., 2020). It exhibits numerous health benefits due to its bioactive properties. It has been shown to have cytotoxic, antioxidant, antibacterial, antifungal, neuroprotective and anti-inflammatory activities (Dosoky & Setzer, 2018b, 2018a). Hence, CLEO is preferred in pharmaceutical contexts due to its efficacy in various therapeutic applications.

Non-melanoma skin cancer (NMSC) is the most common form of skin cancer. It primarily includes basal cell carcinoma (BCC) and squamous cell carcinoma (SCC), both originating from the epidermal layer of the skin (Hedberg et al., 2022). Despite a lower metastatic potential than melanoma, NMSC can cause significant local tissue damage if left untreated. Like other cancers, NMSC arises due to genetic mutations and environmental factors that disrupt normal cellular processes, including cell division, differentiation, and apoptosis. Commonly disrupted regulatory genes in cancers include tumour suppressor genes like *TP53*, proto-oncogenes such as *RAS*, and DNA repair genes, for example, *BRCA1* and *BRCA2* (Sinkala, 2022). Among these, the *TP53* gene plays a pivotal role as a tumour suppressor by regulating the cell cycle, inducing apoptosis, and maintaining genomic stability (Zhu et al., 2020). The *TP53* gene encodes the p53 protein, a tumour suppressor. One of the key functions of p53 protein is detecting DNA damage, halting the cell cycle, initiating DNA repair and triggering apoptosis of extensively damaged cells which are beyond repair (Benjamin & Ananthaswamy, 2007; Marei et al., 2021; Page et al., 2016). On the other hand, these protective roles are impaired in mutated or inactivated p53 proteins. It is important to note that *TP53* are very sensitive to ultraviolet (UV), and mutated *TP53* is a common finding in NMSC (Benjamin & Ananthaswamy, 2007; Paulo et al., 2019). In this circumstance, the skin cells can no longer repair the defective DNA or undergo apoptosis; instead, they continue the cell cycle and proliferate, resulting in cancer (Benjamin & Ananthaswamy, 2007).

Currently, there are various treatments offered for those diagnosed with NMSC, including surgical excision, chemotherapy, radiotherapy and immunotherapy. Nevertheless, current therapies have their own limitations and undesirable effects, such as anaemia, infections, fatigue and others (Sol et al., 2024). Therefore, natural remedies have become a point of interest for researchers seeking to develop treatments for skin cancer. Exposure to EO may affect the activity and expression of p53, potentially reducing tumour cell proliferation and promoting apoptosis, making it an important target for cancer treatment. A study showed that CLEO had cytotoxic effects on human skin, gastric, and brain cancer cells, indicating its anti-proliferative activity (Manjunath & Mahurkar, 2021). Tea tree EO used in previous studies has also been shown to successfully induce apoptosis in human melanoma and squamous cell carcinoma cells by upregulating p53 gene expression (Ramadan et al., 2019). Although direct studies on the effects of CLEO on p53 expression in NMSC are limited, the general anti-cancer mechanisms of citrus EO suggest a possible interaction with pathways involving p53. However, to date, no commercial drugs

based on CLEO have been explicitly approved for the treatment of skin cancer.

The objective of this study is to evaluate the cytotoxic effects of CLEO in NMSC. Specifically, the study seeks to evaluate the morphological changes, p53 protein expression and secretion, and *TP53* gene expression in NMSC treated with CLEO. The findings of this study would contribute to understanding the anticancer effects of CLEO in normal and cancerous skin cells, thereby exploring its potential anticancer role in skin cancer.

MATERIALS AND METHODS

Materials

Reagents and chemicals used in this study were procured from Sigma-Aldrich (St. Louis, MO, United States).

Cell Culture

Human foreskin fibroblast cells (HFF1) and human epidermoid squamous carcinoma cells (A431) were acquired from Shanghai iCell Biotechnology Co., Ltd. These cells were cultured in Dulbecco's Modified Eagle's Medium (DMEM) (Biosera, France) with 10% fetal bovine serum (FBS) (Biosera, France) and 100 IU/mL penicillin-streptomycin (Thermo-Fisher Scientific, USA) in a 75 cm^2 culture flask. The cells were grown in a humidified incubator at 37°C and 5% CO_2. Once they were 80-90% confluent, the cells were subcultured in new flasks following the standard cell culture protocols (Anuar et al., 2024).

Cell morphology study and cell harvesting

The HFF1 and A431 cells were seeded at a density of 3.0×10^5 cells per well in 6-well plates. The cells were then incubated under the conditions described earlier. After 72 hours of incubation, the cells were treated with CLEO dissolved in dimethyl sulfoxide (DMSO) for 24 hours. The cells were treated with 125, 250, and 500 µg/mL CLEO, with each treatment performed in triplicate (three wells per group). The final DMSO concentration was maintained at 0.1% across all treatment groups. Cells treated with 0.1% DMSO (vehicle-treated) served as the negative control. To prepare the CLEO treatment, CLEO was first mixed with DMSO, and the mixture was vortexed until homogenised. A single batch of CLEO was used throughout the study to ensure reproducibility. The 24-hour treatment period is chosen because it provides sufficient time to observe the initial apoptotic response in many cell lines. It was reported that the increase in caspase-3 and cytochrome c levels in ovarian cancer cells, indicative of early apoptotic events, was evident within 24 hours of treatment with resveratrol and nutlin-3 (Marimuthu et al., 2011). Similarly, the cytotoxic effects of dieckol on prostate cancer cells were manifested within 24 hours of treatment, as shown by reactive oxidative species generation and increased apoptotic signals (Karuppaiya et al., 2024).

Next, the cells' morphological changes were qualitatively assessed. Images were captured at 10- to 20-times magnification using an inverted light microscope (Olympus, Japan). Morphological assessment was based on established hallmarks of apoptosis. Apoptotic HFF1 cells were characterised by observable cell rounding compared to their original elongated, spindle-like shape, detachment and a partial loss of cell clustering. On the other hand, apoptotic A431 cells exhibited loss of their original polygonal shape, detachment, and reduced clustering.

After imaging, adherent cells were harvested using TRIzol reagent (Thermo Scientific, USA) and mechanical scraping (Biosera, France). Lastly, the cell lysates were stored at -20°C for subsequent protein and gene expression analyses, and the culture media were preserved at -20°C for protein secretion studies.

Total RNA and protein expression extraction from cell lysate

Firstly, total RNA was extracted from the cell lysates in TRIzol reagent (Thermo Scientific, USA) using the innuPREP RNA Mini Kit (Analytik

Jena) according to the manufacturer's instructions. Then, the extracted RNA was eluted in 30 µl of elution buffer and stored it at -80°C. Protein was isolated from the second filtrate obtained during the RNA extraction process using a cold acetone precipitation method. Lastly, the resulting protein pellets were dissolved in 30 µl of RIPA extraction and lysis buffer, and stored at -20°C for further analysis.

Protein extraction from conditioned media

The collected culture media were mixed with four volumes of 100% cold acetone and incubated at -20°C for 1 hour. Next, the mixture was centrifuged at 13,000 g in an ultracentrifuge (Beckman Coulter Life Sciences, USA) according to the protocol (Mohd Radzuan, 2020). After centrifugation, the resulting protein pellets were air-dried. Then, the pellets were resuspended in 200 µl of RIPA extraction and lysis buffer (Thermo Scientific, USA). The resuspended protein was stored at -20°C for further analysis.

Western blot

Cytosolic protein expression was analysed separately from protein in the media for protein secretion assays. A431 cells treated with 125 µg/mL cisplatin served as the positive control group. The cytosolic and secreted protein extract concentrations were quantified using a Protein Assay BCA Kit (Nacalai Tesque, Japan). For analysis, 50 µg of denatured protein samples were loaded in 2x Laemmli (BioRad, USA) onto a 10% acrylamide gel (BioRad, USA) along with a protein molecular weight marker (BioRad, USA) in the first well. Normalisation to a housekeeping protein was not performed, as conventional intracellular loading controls are absent from the secretome under non-lytic conditions. Electrophoresis was conducted at 100V for 10 minutes, followed by 120V for 1 hour.

After electrophoresis, the protein band on the gel was transferred to a PVDF membrane using the Trans-Blot Turbo Kit (BioRad, USA) at 13V for 20 minutes. Subsequently, the membrane was blocked with 1% bovine serum albumin (BSA) at room temperature for 1 hour. For the protein expression assay, the membrane was cut between 42 and 53 kDa, corresponding to the protein molecular weight marker. Next, the membranes were incubated overnight at 4°C with p53 antibody (sc-263, Santa Cruz Biotechnology, USA) and *ACTB* antibody (C4, Santa Cruz Biotechnology, USA) at a 1:1000 dilution. The following day, the membranes were incubated with a secondary antibody (m-IgG2a BP-HRP: sc-542731, Santa Cruz Biotechnology, USA) at a 1:25 dilution at room temperature for 1 hour. Finally, the protein bands were detected using the Chemi-Lumi One Series for HRP (Nacalai Tesque, Japan). The signals were captured and quantified using the ChemiDoc Imaging System Machine and ChemiDoc XRS software (BioRad, USA).

cDNA conversion

The total RNA concentration for each sample was measured using a NanoDrop 1000 Spectrophotometer (Thermo Scientific, USA). Then, one µg of RNA was used to synthesise 20 µl of cDNA with the SensiFAST™ cDNA Synthesis Kit (BioLine, UK). Finally, the resulting cDNA was stored at -20°C until further analysis.

Gene expression study

First, gene expression analysis was performed using predesigned primers and probes for the *TP53* and *ACTB* genes (IDT DNA, USA). The primer sequences used were as follows: *ACTB*-F (ACAGAGCCTCGCCTTTG), *ACTB*-R (CCTTGCACATGCCGGAG), *ACTB* probe (/56-FAM/TCATCCATG/ZEN/GTGAGCTGGCGG/3IABkFQ/); *TP53*-F (CAAGCAGTCACAGCACATGA), *TP53*-R (AATACTCCACACGCAAATTTCC), and *TP53* probe (56-FAM/CCTCCTCAG/ZEN/CATCTTATCCGAGTGGA/3IABkFQ/).

Next, a 10 µL PCR reaction mixture was prepared by mixing 20x primers and probes, PrimeTime™ Gene Expression Master Mix 2x (IDT DNA, USA), cDNA diluted 1:10, and RNase-free water. Each sample was run in

duplicates. Amplification was carried out using the CFX96 Touch Real-Time PCR Detection System (BioRad, USA) under the following conditions: polymerase activation at 95°C for 3 minutes, denaturation at 95°C for 15 seconds, and annealing/extension at 58°C for 1 minute, repeated for 50 cycles. Data from two biological replicates are presented as mean ± SEM.

Statistical analyses

The CFX Manager™ software (Bio-Rad, USA) was used to calculate relative gene expression (fold-change) in gene expression (ΔΔCq). For this analysis, the fold-change data from three independent biological replicates (each with technical duplicates) were analysed using a one-way ANOVA followed by Tukey's post-hoc test (comparing all treatments to the vehicle control). A p-value < 0.05 was considered significant.

RESULTS

Effect of CLEO on Cell Morphology

In the morphologic study, untreated and DMSO-treated HFF1 cells exhibited typical fibroblast-like morphology, with elongated spindles and intact cellular structures (Figure 1, A-B). However, treatment with CLEO at concentrations of 125 µg/mL and 250 µg/mL for 24 hours induced observable morphological changes (Figure 1, C-E). At these concentrations, some cells showed slight rounding and reduced adherence. Despite these changes, the majority of cells retained their overall structure, and the alterations were less pronounced compared to those observed in cancerous A431 cells.

In contrast, A431 cells showed noticeable changes following CLEO treatment. The untreated control and DMSO-treated

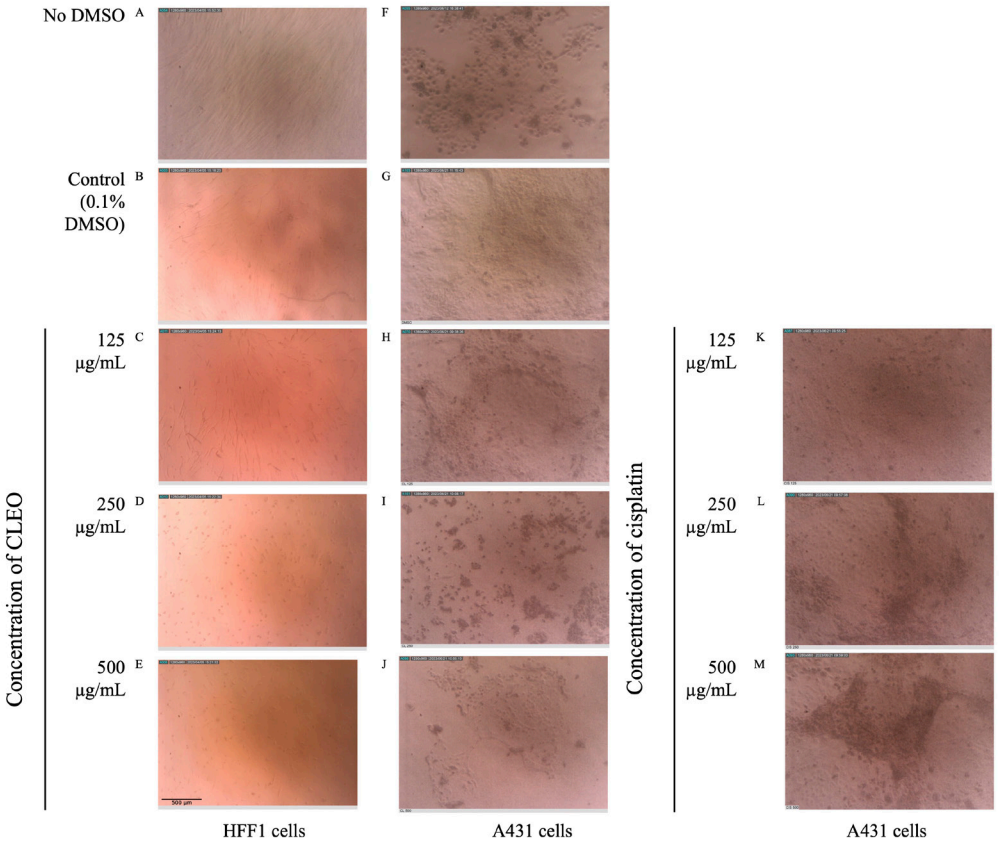

Figure 1: The overall morphological impact of CLEO treatment on cell density and confluence at a population level in HFF1 cells (A-E) and A431 cells (F-J) after 24 h of treatment with CLEO, and cisplatin (K-M). Cells were observed under 20x magnification. CLEO = Citrus lemon essential oil. Scale bar: 500 µm (based on standard 20x field of view).

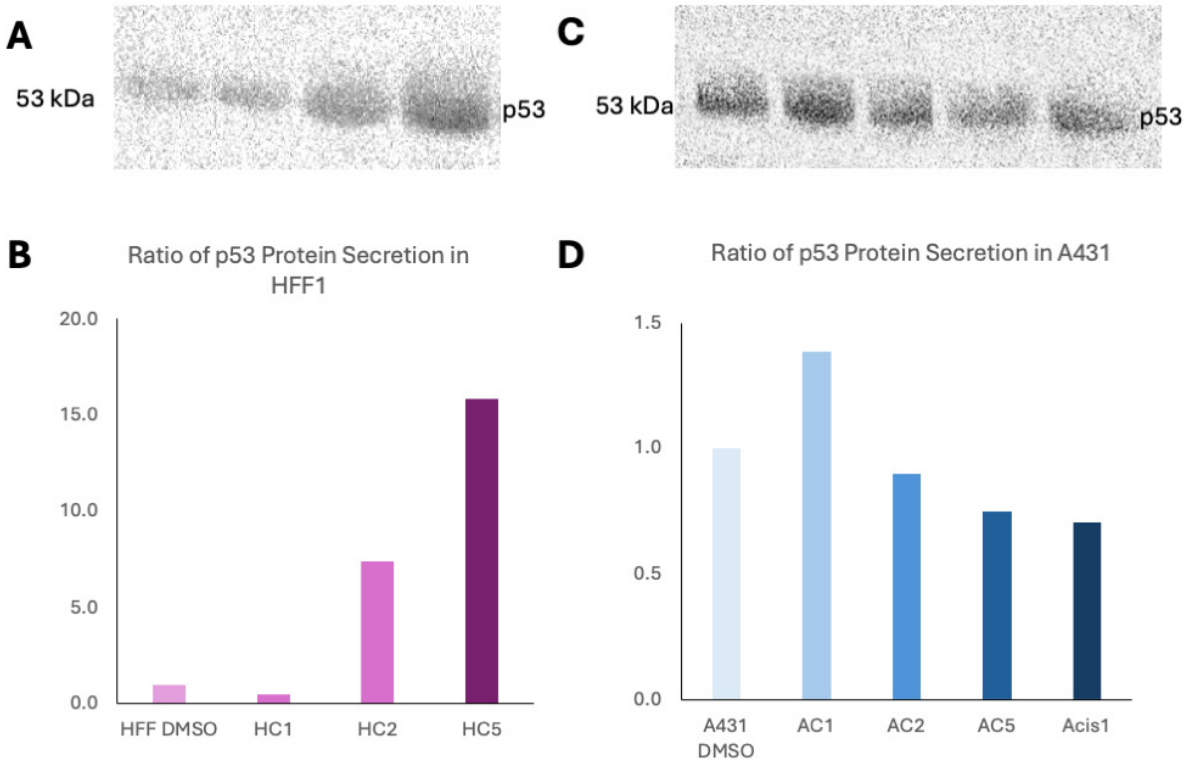

Figure 2: Analysis of (secreted) p53 protein levels in cell culture media. A) Western blot image of p53 protein secretion in HFF1 cells of different treatments (vehicle (0.1% DMSO) as control, 125 µg/mL CLEO, 250 µg/mL CLEO, and 500 µg/mL CLEO) and B) its densitometric ratio compared to control (vehicle-treated), normalised to equal volume loading. C) Western blot image of p53 protein secretion in A4311 cells of different treatments (vehicle (0.1% DMSO) as control, 125 µg/mL CLEO, 250 µg/mL CLEO, 500 µg/mL CLEO and 125 µg/mL cisplatin) and D) its densitometric ratio compared to control (vehicle-treated), normalised to equal volume loading. Equal volumes of concentrated conditioned media were loaded for all samples; normalisation to a housekeeping protein was not applicable for secretome analysis. Acis1 = A431 cells treated with 125 µg/mL cisplatin; A431DMSO = A431 cells treated with 0.1% DMSO; AC1 = A431 cells treated with 125 µg/mL CLEO; AC2 = A431 cells treated with 250 µg/mL CLEO; AC5 = A431 cells treated with 500 µg/mL CLEO; HFF1DMSO = HFF1 cells treated with 0.1% DMSO, HC1 = HFF1 cells treated with 125 µg/mL CLEO; HC22 = HFF1 cells treated with 250 µg/mL CLEO; HC5 = HFF1 cells treated with 500 µg/mL CLEO.

cells displayed typical epithelial morphology with high cell density and intact structures (Figure 1, F-G). However, treatment with CLEO and cisplatin at concentrations of 125, 250, and 500 µg/mL for 24 hours resulted in significant morphological alterations, including cell shrinkage, membrane blebbing, and detachment, particularly at higher concentrations (Figure 1, H-M).

Effect of CLEO on p53 Protein Expression and Secretion

Cytosolic protein concentrations for HFF1 and A431 cells were below the detection threshold for reliable quantification. Western blot analysis for p53 protein secretion was performed. Due to sample availability constraints, this analysis was conducted on a single biological replicate per condition. The data are therefore presented as observed fold-changes and should be considered preliminary. HFF1 cells treated with 500 µg/mL CLEO had the highest secreted p53 (16-fold), followed by 250 µg/mL (7.5-fold), and 125 µg/mL (0.5-fold) (Figure 2, A-B).

Meanwhile, A431 cells treated with

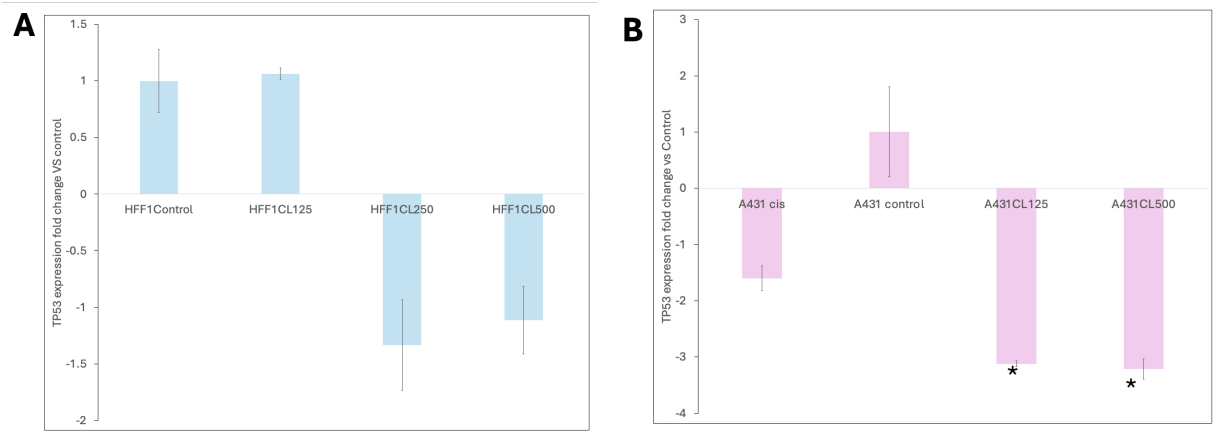

Figure 3: Relative *TP53* expression fold change vs control in A) HFF1 cells and B) A431 cells after treatment with CLEO at 125, 250 and 500 µg/mL for 24 h. * indicates significant $p<0.05$ compared to control. A431 cis = A431 cells treated with 125 µg/mL cisplatin; A431Control = A431 cells treated with 0.1% DMSO; A431CL125 = A431 cells treated with 125 µg/mL CLEO; A431CL500 = A431 cells treated with 500 µg/mL CLEO; HFF1CL125 = HFF1 cells treated with 125 µg/mL CLEO; HFF1CL250 = HFF1 cells treated with 250 µg/mL CLEO; HFF1CL500 = HFF1 cells treated with 500 µg/mL CLEO; HFF1Control = HFF1 cells treated with 0.1% DMSO..

125 µg/mL CLEO showed the highest secretion of p53 protein, followed by control, 250 µg/mL CLEO, and 500 µg/mL CLEO (Figure 2, C-D). A431 cells treated with 125 µg/mL CLEO showed a 1.4-fold increase compared to the control (1-fold). For A431 cells treated with 250 µg/mL CLEO, the CLEO concentration was 0.5-fold, and for A431 cells treated with 500 µg/mL CLEO, the CLEO concentration was 0.75-fold compared to the control.

Effect of CLEO on *TP53* Gene Expression

There were no significant changes in *TP53* gene expression in CLEO-treated HFF1 cells compared to control (Figure 3A). In contrast, analysis of the *TP53* gene in A431 treated with 125 and 500 µg/mL of CLEO exhibited a significant downregulation compared to control ($p<0.001$, respectively) (Figure 3B). RNA yield in A431 cells treated with 250 µg/mL of CLEO was below the detection threshold for reliable quantification of *TP53* gene expression.

DISCUSSION

Citrus limon is extensively utilised across diverse industries due to its versatile applications. CLEO, previously shown to have various health benefits, was studied in depth to assess its potential for treating cancers, including skin cancer. This study examined cell morphology, p53 protein secretion, and *TP53* gene expression to better understand the cytotoxic mechanisms by which CLEO differentially affects normal and cancerous skin cells.

We observed that higher concentrations of CLEO caused mild morphological changes in normal HFF1 cells. The morphological changes are suggestive of early signs of cellular stress or cytotoxicity. In contrast, A431 cancer cells treated with CLEO showed significant morphological changes, including loss of the original polygonal shape, cell detachment, and reduced clustering. These observed changes were dose-dependent, with more pronounced changes at higher CLEO concentrations. The changes in the cellular morphology are highly likely due to the oxidative stress and disrupted membrane integrity, induced by the bioactive compounds present in CLEO, for example, limonene and citral (Gautam et al., 2014; Manjunath & Mahurkar, 2021). It is noteworthy that HFF1 cells showed greater resilience to CLEO than A431 cells. A plausible mechanism is that the further insult by the CLEO bioactive compounds on top of the defective or dysfunctional *TP53* genes in A431 cells triggers another mechanism leading to cell apoptosis or necrosis (Cordani et al., 2016; Ozaki & Nakagawara, 2011). Meanwhile,

normal HFF1 cells with functional *TP53* could repair DNA more effectively, leading to less cell death than A431 cancer cells. Hence, HFF1 demonstrated superior resistance to cellular stress. Nevertheless, it is important to optimise the CLEO dose to minimise adverse effects on normal cells. We acknowledged that, in future studies, a formal, blinded scoring system should be employed to assess morphological changes and reduce bias in assessment and improve objectivity.

The second objective of this study was to evaluate the effect of CLEO on p53 secretion and *TP53* expression in skin cancer cells. There was a contrasting trend in these parameters between the normal HFF1 and A431 cancer cell lines. In normal HFF1 cells, there was higher p53 protein secretion in cells treated with higher CLEO concentrations. One possible inference is that higher p53 secretion could be a stress response to cellular insults induced by the CLEO. The bioactive compounds in CLEO are foreign to cells, thereby triggering inflammatory responses and leading to apoptosis or senescence (Hafner et al., 2019; Yu et al., 2006). Surprisingly, the cancerous A431 cells had reduced p53 protein secretion at higher CLEO concentrations in contrast to HFF1 cells. As explained earlier, A431 cells are likely to have a defective *TP53* gene and a reduced capacity to cope with cellular stress. Further insult and oxidative damage from exposure to CLEO may cause a greater degree of damage, destabilisation, and defects in the p53 proteins (Møller et al., 2007). Another plausible explanation for this observation is that the p53 antibody used in the Western Blot in this study is designed to bind wild-type p53 rather than the defective p53 synthesised by A431 cells. At higher CLEO concentrations, there was further damage to the cells' DNA, leading to a lower amount of normal, functional p53 proteins being secreted. CLEO may induce oxidative damage and impair TP53 gene expression and p53 protein stability via multiple mechanisms. For example, oxidation of cysteine and methionine residues can disrupt p53 structural integrity and zinc binding (Nomura et al., 2009; Scotcher et al., 2013). Additionally, oxidative stress modulates MDM2 activity and promotes post-translational modifications such as phosphorylation and crotonylation, further influencing p53 degradation (Lee et al., 2008; Liao et al., 2020). Natural compounds may also directly interact with the p53-MDM2 pathway or induce reactive oxygen species, altering p53 stability in a context-dependent manner (Qin et al., 2018; Ramli et al., 2024).

Furthermore, downregulation of *TP53* gene expression was observed in CLEO-treated A431 cells at 125 and 500 µg/mL. However, a notable limitation in the dose-response analysis in this study was insufficient RNA yield from A431 cells treated with the intermediate CLEO concentration of 250 µg/mL, preventing reliable quantification. As a result, a complete assessment of the concentration-dependent effect was not possible. Despite this gap, the consistent downregulation at the two effective concentrations, 125 and 500 µg/mL, suggests a potential role for p53 in CLEO's mechanism of action in A431 cells. This effect appears to be cell-type-specific since it was not observed in HFF1 cells, which remained unaffected at all CLEO doses. This observation points to the selective targeting of CLEO to cancer cells, a desirable characteristic for a potential therapeutic agent. Overall, our findings were contrary to the expected upregulation as observed in previous studies. We proposed that CLEO could have induced other alternative p53-independent pathways that eventually lead to apoptosis of the cancer cells, as suggested by previous studies (Srivastava et al., 2012; Yoon et al., 2024). This warrants further studies to investigate the possible pathways affected by CLEO.

Our current qPCR data measure steady-state mRNA levels. At this level, it is not possible to distinguish whether the low mRNA level is due to transcriptional repression or to mRNA degradation. The observed downregulation of *TP53* mRNA and reduced extracellular p53 levels at higher CLEO concentrations in A431 cells certainly raises important mechanistic questions. This observed CLEO effect is unlikely

to be due solely to cytotoxicity, as it was also apparent at concentrations that had only modest effects on cell morphology. Moreover, it was not evident in the equally sensitive HFF1 cells. Possible reasons include CLEO-induced repression of *TP53* transcription or promotion of *TP53* mRNA degradation. Furthermore, CLEO could have induced post-translational modifications, destabilising the p53 protein, which eventually renders it a target for proteasomal degradation. To uncover the underlying mechanisms of CLEO's cell-type-specific effects on *TP53*/p53 dynamics, future studies should employ nuclear run-on assays, mRNA stability analyses, and analysis of p53 protein half-life. Although significant cell death at higher concentrations could be a major confounding factor, our data suggest that cell death is not the sole explanation for *TP53* downregulation in A431 cells treated with a higher CLEO concentration. The non-malignant HFF1 cells showed no significant change in *TP53* expression despite the highest concentrations. This suggests that the downregulation in A431 cells is not merely a general consequence of cell death but may involve a mechanism specific to the cancer cell line. Further studies to clarify the molecular pathways are warranted by analysing the apoptotic and autophagic markers and p53 mutational status in these CLEO-treated cells.

CONCLUSION

CLEO is cytotoxic towards in vitro skin cancer cells in a dose-dependent manner. While it activates p53 mechanisms in normal skin cells, CLEO activates alternative p53-independent cytotoxic mechanisms in skin cancer cells. Overall, this study suggests the potential of CLEO, a natural compound, as a complementary therapy for non-melanoma skin cancer, targeting cancer cells with minimal toxicity to normal cells. However, further investigations are needed to elucidate the precise molecular pathways involved in CLEO-induced cytotoxicity in skin cancer cells. This is essential for optimising the therapeutic application of CLEO while minimising its impact on normal cells.

CONFLICT OF INTEREST

There was no conflict of interest.

ACKNOWLEDGEMENT

International Islamic University Malaysia funded this study through the Research Management Centre Grant 2020 (RMCG20-020-0020). We want to acknowledge the Department of Basic Medical Sciences, Kulliyyah of Medicine, International Islamic University Malaysia, for providing access to laboratory facilities and other materials to conduct this study.

REFERENCES

Anuar, M. A. F., Zamani, M. R., Aminuddin, A. H., Omar, W. F. N. W., & Radzuan, H. Mohd. (2024). Cytotoxic Effects of Cananga odorata Essential Oil on p53 Protein and TP53 Gene Dynamics in Non-Melanoma Skin Cancer. Journal of Environmental Microbiology and Toxicology, 12(2), 25–30. https://doi.org/10.54987/jemat.v12i2.1009

Benjamin, C. L., & Ananthaswamy, H. N. (2007). p53 and the pathogenesis of skin cancer. Toxicology and Applied Pharmacology, 224(3), 241–248. https://doi.org/10.1016/J.TAAP.2006.12.006

Cordani, M., Pacchiana, R., Butera, G., D'Orazi, G., Scarpa, A., & Donadelli, M. (2016). Mutant p53 proteins alter cancer cell secretome and tumour microenvironment: Involvement in cancer invasion and metastasis. Cancer Letters, 376(2), 303–309. https://doi.org/10.1016/J.CANLET.2016.03.046

Dosoky, N. S., & Setzer, W. N. (2018a). Biological Activities and Safety of Citrus spp. Essential Oils. International Journal of Molecular Sciences, 19(7). https://doi.org/10.3390/IJMS19071966

Dosoky, N. S., & Setzer, W. N. (2018b). Chemical Composition and Biological Activities of Essential Oils of Curcuma Species. Nutrients, 10(9). https://doi.org/10.3390/NU10091196

Gautam, N., Mantha, A. K., & Mittal, S. (2014). Essential oils and their constituents as anticancer agents: a mechanistic view.

BioMed Research International, 2014. https://doi.org/10.1155/2014/154106

Hafner, A., Bulyk, M. L., Jambhekar, A., & Lahav, G. (2019). The multiple mechanisms that regulate p53 activity and cell fate. Nature Reviews Molecular Cell Biology 2019 20:4, 20(4), 199–210. https://doi.org/10.1038/s41580-019-0110-x

Hedberg, M. L., Berry, C. T., Moshiri, A. S., Xiang, Y., Yeh, C. J., Attilasoy, C., Capell, B. C., & Seykora, J. T. (2022). Molecular Mechanisms of Cutaneous Squamous Cell Carcinoma. International Journal of Molecular Sciences 2022, Vol. 23, Page 3478, 23(7), 3478. https://doi.org/10.3390/IJMS23073478

Karuppaiya, V., Annamalai, A., Krishnamurthy, S., & Soundarapandian, K. (2024). Dieckol prevents prostate cancer cell proliferation by transcriptionally attenuating JAK/STAT3 signaling pathway. Environmental Toxicology, 39(3), 1187–1196. https://doi.org/10.1002/TOX.24006

Klimek-szczykutowicz, M., Szopa, A., & Ekiert, H. (2020). Citrus limon (Lemon) Phenomenon-A Review of the Chemistry, Pharmacological Properties, Applications in the Modern Pharmaceutical, Food, and Cosmetics Industries, and Biotechnological Studies. Plants (Basel, Switzerland), 9(1). https://doi.org/10.3390/PLANTS9010119

Lee, J. H., Jeong, M. W., Kim, W., Yoon, H. C., & Kim, K. T. (2008). Cooperative Roles of c-Abl and Cdk5 in Regulation of p53 in Response to Oxidative Stress. Journal of Biological Chemistry, 283(28), 19826–19835. https://doi.org/10.1074/JBC.M706201200

Liao, P., Bhattarai, N., Cao, B., Zhou, X., Jung, J. H., Damera, K., Fuselier, T. T., Thareja, S., Wimley, W. C., Wang, B., Zeng, S. X., & Lu, H. (2020). Crotonylation at serine 46 impairs p53 activity. Biochemical and Biophysical Research Communications, 524(3), 730–735. https://doi.org/10.1016/J.BBRC.2020.01.152

Manjunath, C., & Mahurkar, N. (2021). In vitro cytotoxicity of cardamom oil, lemon oil, and jasmine oil on human skin, gastric, and brain cancer cell line. Journal of Cancer Research and Therapeutics, 17(1), 62–68. https://doi.org/10.4103/JCRT.JCRT_915_17

Marei, H. E., Althani, A., Afifi, N., Hasan, A., Caceci, T., Pozzoli, G., Morrione, A., Giordano, A., & Cenciarelli, C. (2021). p53 signaling in cancer progression and therapy. Cancer Cell International, 21(1), 703. https://doi.org/10.1186/s12935-021-02396-8

Marimuthu, P., Kaur, K., Kandalam, U., Jasani, V., Bukhari, N., Nguyen, M., Abdul, A., Pervez, F. F., & Rathinavelu, A. (2011). Treatment of Ovarian Cancer Cells with Nutlin-3 and Resveratrol Combination Leads to Apoptosis via Caspase Activation. Https://Home.Liebertpub.Com/Jmf, 14(1–2), 46–52. https://doi.org/10.1089/JMF.2009.0270

Mohd Radzuan, H. (2020). The Effect of Obesogenic and Inflammatory Factors in Regulating Adipocytes Lipid Chaperone Proteins [PhD Thesis, University of Nottingham]. https://eprints.nottingham.ac.uk/id/eprint/59800

Møller, I. M., Jensen, P. E., & Hansson, A. (2007). Oxidative modifications to cellular components in plants. Annual Review of Plant Biology, 58(Volume 58, 2007), 459–481. https://doi.org/10.1146/ANNUREV.ARPLANT.58.032806.103946/1-PDF

Nomura, T., Kamada, R., Ito, I., Chuman, Y., Shimohigashi, Y., & Sakaguchi, K. (2009). Oxidation of methionine residue at hydrophobic core destabilizes p53 tetrameric structure. Biopolymers, 91(1), 78–84. https://doi.org/10.1002/BIP.21084

Ozaki, T., & Nakagawara, A. (2011). Role of p53 in Cell Death and Human Cancers. Cancers, 3(1), 994. https://doi.org/10.3390/CANCERS3010994

Page, A., Navarro, M., Suarez-Cabrera, C., Alameda, J. P., Casanova, M. L., Paramio, J. M., Bravo, A., & Ramirez, A. (2016). Protective role of p53 in skin cancer: Carcinogenesis studies in mice lacking epidermal p53. Oncotarget, 7(15), 20902–20918. https://doi.org/10.18632/oncotarget.7897

Paulo, M. S., Adam, B., Akagwu, C., Akparibo, I., Al-Rifai, R. H., Bazrafshan, S., Gobba, F., Green, A. C., Ivanov, I., Kezic, S., Leppink, N., Loney, T., Modenese, A., Pega, F., Peters, C. E., Prüss-Üstün, A. M., Tenkate, T., Ujita, Y., Wittlich, M., & John, S. M. (2019). WHO/ILO work-related burden of disease and injury: Protocol for systematic reviews of occupational exposure to solar ultraviolet radiation and of the effect of occupational exposure to solar ultraviolet radiation on melanoma and non-melanoma skin cancer. Environment International, 126, 804–815. https://doi.org/10.1016/J.ENVINT.2018.09.039

Qin, J. J., Li, X., Hunt, C., Wang, W., Wang, H., & Zhang, R. (2018). Natural products targeting the p53-MDM2 pathway and mutant p53: Recent advances and implications in cancer medicine. Genes & Diseases, 5(3), 204–219. https://doi.org/10.1016/J.GENDIS.2018.07.002

Ramadan, M. A., Shawkey, A. E., Rabeh, M. A.,

& Abdellatif, A. O. (2019). Expression of P53, BAX, and BCL-2 in human malignant melanoma and squamous cell carcinoma cells after tea tree oil treatment in vitro. Cytotechnology, 71(1), 461–473. https://doi.org/10.1007/S10616-018-0287-4

Ramli, I., Cheriet, T., Posadino, A. M., Giordo, R., Fenu, G., Nwachukwu, K. C., Oyewole, O. A., Adetunji, C. O., Calina, D., Sharifi-Rad, J., & Pintus, G. (2024). Modulating the p53-MDM2 pathway: The therapeutic potential of natural compounds in cancer treatment. EXCLI Journal, 23, 1397–1439. https://doi.org/10.17179/EXCLI2024-7791

Scotcher, J., Clarke, D. J., MacKay, C. L., Hupp, T., Sadler, P. J., & Langridge-Smith, P. R. R. (2013). Redox regulation of tumour suppressor protein p53: identification of the sites of hydrogen peroxide oxidation and glutathionylation. Chemical Science, 4(3), 1257–1269. https://doi.org/10.1039/C2SC21702C

Sinkala, M. (2022). Mutational Landscape of Cancer-Driver Genes Across Human Cancers. BioRxiv, 2022.09.11.507448. https://doi.org/10.1101/2022.09.11.507448

Sol, S., Boncimino, F., Todorova, K., Waszyn, S. E., & Mandinova, A. (2024). Therapeutic Approaches for Non-Melanoma Skin Cancer: Standard of Care and Emerging Modalities. International Journal of Molecular Sciences, 25(13). https://doi.org/10.3390/IJMS25137056

Srivastava, P., Yadav, N., Lella, R., Schneider, A., Jones, A., Marlowe, T., Lovett, G., O'Loughlin, K., Minderman, H., Gogada, R., & Chandra, D. (2012). Neem oil limonoids induces p53-independent apoptosis and autophagy. Carcinogenesis, 33(11), 2199. https://doi.org/10.1093/CARCIN/BGS269

Yoon, Y. E., Jung, Y. J., & Lee, S. J. (2024). The Anticancer Activities of Natural Terpenoids That Inhibit Both Melanoma and Non-Melanoma Skin Cancers. International Journal of Molecular Sciences, 25(8). https://doi.org/10.3390/IJMS25084423

Yu, X., Harris, S. L., & Levine, A. J. (2006). The Regulation of Exosome Secretion: a Novel Function of the p53 Protein. Cancer Research, 66(9), 4795–4801. https://doi.org/10.1158/0008-5472.CAN-05-4579

Zhu, G., Pan, C., Bei, J. X., Li, B., Liang, C., Xu, Y., & Fu, X. (2020). Mutant p53 in Cancer Progression and Targeted Therapies. Frontiers in Oncology, 10, 595187. https://doi.org/10.3389/FONC.2020.595187/XML/NLM